

Intrinsic and interfacial effect of electrode metals on the resistive switching behaviors of zinc oxide films

This content has been downloaded from IOPscience. Please scroll down to see the full text.

2014 Nanotechnology 25 425204

(<http://iopscience.iop.org/0957-4484/25/42/425204>)

View [the table of contents for this issue](#), or go to the [journal homepage](#) for more

Download details:

IP Address: 210.72.19.250

This content was downloaded on 01/11/2015 at 07:22

Please note that [terms and conditions apply](#).

Intrinsic and interfacial effect of electrode metals on the resistive switching behaviors of zinc oxide films

W H Xue^{1,3,4}, W Xiao², J Shang^{1,4}, X X Chen^{1,4}, X J Zhu^{1,4}, L Pan^{1,4},
H W Tan^{1,4}, W B Zhang^{1,4}, Z H Ji^{1,4}, G Liu^{1,4}, X-H Xu³, J Ding^{1,2,4} and
R-W Li^{1,4}

¹ Key Laboratory of Magnetic Materials and Devices, Ningbo Institute of Materials Technology and Engineering, Chinese Academy of Sciences, Ningbo 315201, People's Republic of China

² Department of Materials Science and Engineering, National University of Singapore, 119260, Singapore

³ Key Laboratory of Magnetic Molecules and Magnetic Information Materials of Ministry of Education, School of Chemistry and Materials Science, Shanxi Normal University, Linfen 041004, People's Republic of China

⁴ Zhejiang Province Key Laboratory of Magnetic Materials and Application Technology, Ningbo Institute of Materials Technology and Engineering, Chinese Academy of Sciences, Ningbo 315201, People's Republic of China

E-mail: liug@nimte.ac.cn (Prof. G. Liu), xuxiaohong_ly@163.com (Prof. X.-H. Xu) and msedingj@nus.edu.sg (Prof. J. Ding)


Received 15 April 2014, revised 1 August 2014

Accepted for publication 26 August 2014

Published 2 October 2014

Abstract

Exploring the role of electrode metals on the resistive switching properties of metal electrode/oxide/metal electrode sandwiched structures provides not only essential information to understand the underlying switching mechanism of the devices, but also useful guidelines for the optimization of the switching performance. A systematic study has been performed to investigate the influence of electrodes on the resistive switching characteristics of zinc oxide (ZnO) films in this contribution, in terms of both the intrinsic and interfacial effects. It has been found that the low-resistance state resistances (Ω_{LRS}) of all the investigated devices are below 50 Ω , which can be attributed to the formation of highly conductive channels throughout the ZnO films. On the other hand, the high-resistance state resistances (Ω_{HRS}) depend on the electronegativity and ionic size of the employed electrode metals. Devices with electrode metals of high electronegativity and large ionic size possess high Ω_{HRS} values, while those with electrode metals of low electronegativity and small ionic size carry low Ω_{HRS} values. A similar trend of the set voltages has also been observed, while the reset voltages are all distributed in a narrow range close to ± 0.5 V. Moreover, the forming voltages of the switching devices strongly depend on the roughness of the metal/ZnO and/or ZnO/metal interface. The present work provides essential information for better understanding the switching mechanism of zinc oxide based devices, and benefits the rational selection of proper electrode metals for the device performance optimization.

 Online supplementary data available from stacks.iop.org/NANO/25/425204/mmedia

Keywords: resistive switching, electronegativity, ionic size, roughness

(Some figures may appear in colour only in the online journal)

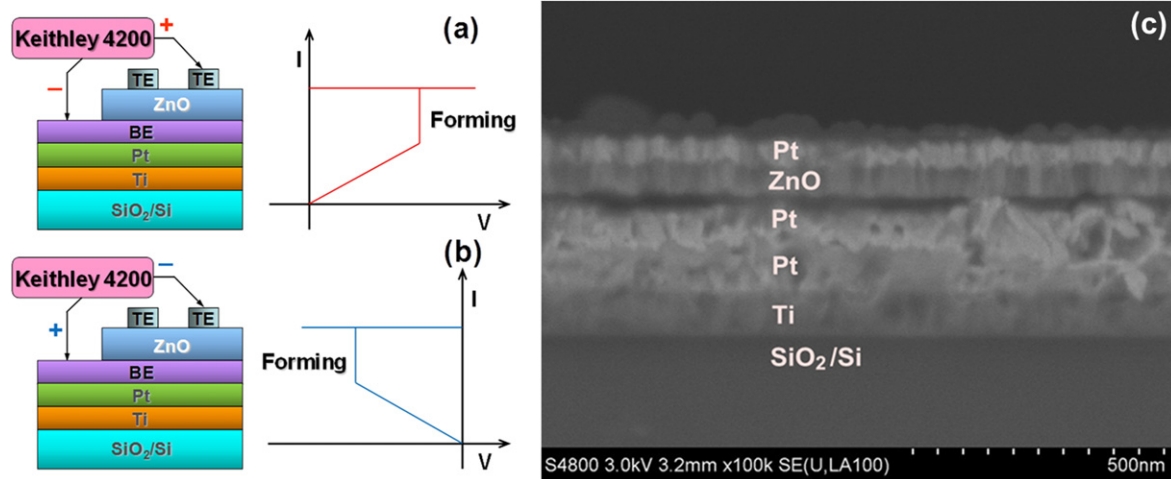


Figure 1. Schematic illustration of the M/ZnO/M symmetric devices samples subjected to (a) positive and (b) negative forming voltages. (c) Cross-sectional SEM image of the as-fabricated Pt/ZnO/Pt device.

1. Introduction

Resistive random access memory (RRAM), which uses the electrically switchable resistance to store digital information, is considered as one of the most promising candidates for the next-generation memories, due to its simple structure, non-destructive readout, fast-speed, low-energy, and high-endurance potential [1–3]. A RRAM device usually consists of an insulator or a semiconductor layer sandwiched between two metal electrodes, where various oxide materials and metal/oxide/metal structures have been intensively explored for resistive switching properties [4–9]. Generally, an electroforming process is required in metal/oxide/metal structures to generate an initial conducting path throughout the oxide matrix that is absent in the virgin devices. With the preformed conduction path, the device can be reversibly set and reset between a high resistance state (HRS) and a low resistance state (LRS).

With its simple stoichiometry, easy preparation and good compatibility with CMOS technology [10–13], zinc oxide (ZnO) has been widely studied as wide-gap semiconductor, transparent electrode, or in optoelectronics, piezoelectrics, spintronics and etc. The resistive switching behaviors of ZnO are also found to be tunable *via* doping and microstructure manipulation [14–28]. Nevertheless, as an integrated and important part of the sandwiched structures, electrodes also play a key role in modulating the switching properties of the devices. For instance, the choice of electrode metals determines the mobile species in the oxide layer and consequently the switching mechanism of the devices [29]. The electrodes which are capable of reserving oxygen ions, or capable of inducing the migration of vacancies inside the oxide layer, can lead to superior bipolar resistive switching behaviors [30–34]. The band alignment between the switching oxide layer and the metal electrodes also controls the interface resistance, which in turn influences the current level, switching power and conduction mechanism of the devices [35]. In addition, the work function, electronegativity,

enthalpy of oxide formation, interfacial roughness and etc of the electrode materials are other typical parameters that may influence the device performance. Unfortunately, less effort has been devoted to the electrode engineering to understand such effect of the electrodes, albeit such intrinsic and interfacial properties of the electrode metals are of equal importance to optimize the device performance. In this work, we have carried out a systematic study to investigate how electrode affects the resistive switching properties of zinc oxide films. Both experimental observation and simulation results suggest that the switching parameters of the zinc oxide based devices, including the forming voltages, set and reset voltages, HRS and LRS resistances, are directly related to the electronegativity and ionic size of the electrode metals, as well as the metal/oxide interfacial roughness at both electrodes. The present findings may provide essential information for better understanding the switching mechanism of zinc oxide based devices, and benefit the rational selection of proper electrode metals for the device performance optimization.

2. Experimental details

Commercially available Pt/Ti/SiO₂/Si substrate was used as the platform for deposition of other metal bottom electrodes (BEs) with good film adhesion. Different metal BEs of platinum (Pt), gold (Au), nickel (Ni), copper (Cu) and silver (Ag) were deposited with the thickness of 30 nm–50 nm at room temperature (RT) by electron beam evaporation technique. Zinc oxide films were fabricated on different BEs through rf magnetron sputtering at RT according to the well-defined procedure [30, 36, 37]. A mixed atmosphere of argon and oxygen (1 Pa, 20% O₂) was maintained during ZnO deposition and the film thickness was fixed as 90 nm to enable resistive switching with a reasonable low leakage current. Top electrodes (TEs) of Pt, Au, Ni, Cu and Ag with a diameter of 100 μm and thickness of 50 nm were deposited through a

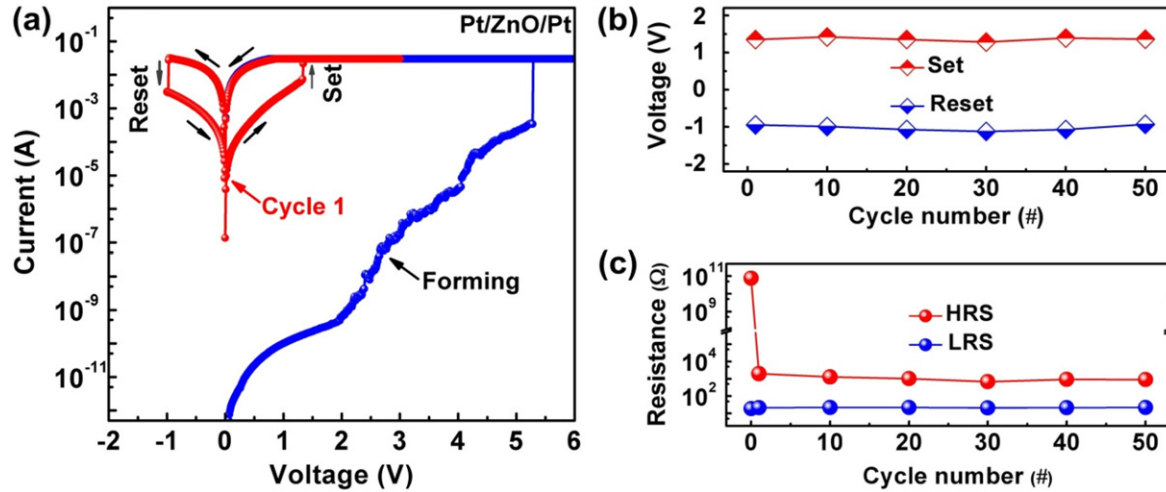


Figure 2. (a) Current–voltage (I – V) characteristics of the positively formed Pt/ZnO/Pt device. The arrows indicate the sweeping directions. Distribution of the (b) set/reset voltages and (c) HRS/LRS resistances of the positively formed Pt/ZnO/Pt device against the switching cycles. The resistances are recorded at a read voltage of 0.1 V.

metal shadow mask onto the ZnO films by electron beam evaporation technique. The metal/ZnO/metal sandwiched structures are illustrated in figures 1(a) and (b). The thickness of ZnO film, Pt TE and Pt BE can be verified by field-emission scanning electron microscopic image (FESEM, Hitachi, S-4800) of figures 1(c) and S1, respectively. The cross-sectional images (layer thickness in particular) of other symmetric devices are similar to that of the Pt/ZnO/Pt devices and are not shown here. The crystalline structure of the as-deposited ZnO films was investigated by grazing-incidence x-ray diffraction technique (Bruker AXS, D8 Discover) using Cu–K α radiation. The incidence angle of x-ray beam was fixed at 1°. All the as-obtained ZnO films are wurtzite, as shown in the XRD pattern of figure S2. The surface morphology of each sample is monitored on a scanning probe microscope (Veeco Dimention 3100 V), which is also equipped with a conducting cantilever coated with Pt/Ir for conductive atomic force microscopic (AFM) measurements of the ZnO/M structures. RT current–voltage (I – V) characteristics of the devices were investigated on a Keithley 4200 semiconductor characterization system with a direct current (dc) voltage sweeping mode. During testing, all the voltages were applied to the TEs, while BEs were kept grounded. The metal/ZnO/metal structures were initially electroformed with either a positive or negative forming voltage (figures 1(a) and (b)), and then swept with both positive and negative biases. Current compliance of 0.03 A was used for the forming and set processes to avoid permanent breakdown of the samples. Resistance of the high and low resistance state (HRS and LRS), Ω_{HRS} and Ω_{LRS} , respectively, were recorded with a read voltage of 0.1 V. Temperature dependence of the device resistances was measured by physical property measurement system (PPMS, Quantum Design) with a conventional two-probe method. A cell was set to LRS with a current compliance of 0.03 A and another was reset to HRS. Then the devices were connected with platinum (Pt) wires using high conductive silver glue, followed by welding of the Pt wires to

the PPMS sample stage. During the RT measurements, a constant-current mode was used with an excitation current of 1 mA.

3. Results and discussion

The forming and subsequent resistive switching processes of a Pt/ZnO/Pt structure are shown in the I – V characteristics of figure 2(a). The initial stage (initial resistance state, or IRS) of the device possesses a high resistance of $7.56 \times 10^{10} \Omega$ (Ω_{IRS}), and a relatively high forming voltage (5.3 V) is required to set the device to the low resistance state (LRS) for the first time. The set and reset voltages are 1.35 V and –0.95 V, respectively, and are almost insensitive to the cycling operations (figure 2(b)). The switching voltages are found to be fluctuated in a very narrow range of $\pm 5\%$. On the other hand, the high resistance state resistance (Ω_{HRS}) decreases with cycling numbers and becomes stable after about 30 cycles, while the low resistance state resistance (Ω_{LRS}) is almost constant as the cycling operation continues (figure 2(c)). To be more accurate and representative, only the stabilized Ω_{HRS} and Ω_{LRS} are used subsequently to study the influence of electrode materials.

Other devices exhibit similar resistive switching characteristics. It is noteworthy that the Ω_{IRS} values for all the devices evaluated in this work are much higher than the Ω_{HRS} obtained after electroforming operation is performed (table S1), which is contributed to insufficient amount of defects present in the virgin oxides [38]. Nevertheless, for any of the so-called symmetric devices whose BE and TE are of the same metal, the Ω_{LRS} value is similar (9 Ω –23 Ω), independent of the electrode materials and demonstrating metallic behavior with positive resistance-temperature coefficient (figures 3(a) and S3). Nevertheless, the conductive AFM analysis reveals that the widely accepted model of formation, rupture and regeneration of the filamentary conduction

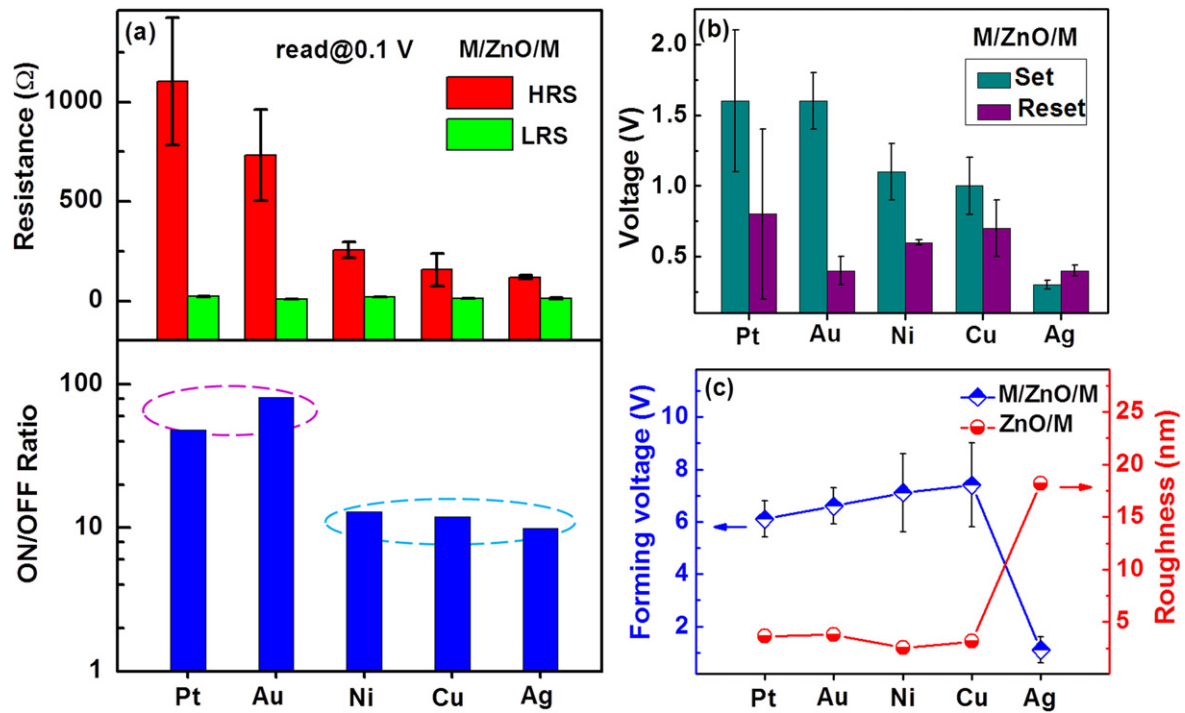


Figure 3. (a) HRS/LRS resistances and ON/OFF ratios, (b) set/reset voltages, (c) forming voltages and surface roughnesses of ZnO films grown on various electrodes. The data point for each electrode was acquired from five random cells with 5 dc cycles and the resistances are recorded at a read voltage of 0.1 V.

Table 1. Electronegativity, work function, atomic radius and ion radius of Pt, Au, Ni, Cu and Ag.

Metal	Pt	Au	Ni	Cu	Ag
Electronegativity [50]	2.2	2.4	1.8	1.9	1.9
Work function (eV) [51]	5.65	5.1	5.15	4.65	4.26
Ion radius (pm) [52]	Pt ²⁺ 94	Au ⁺ 151	Ni ²⁺ 83	Cu ⁺ 91	Ag ²⁺ 94
	—	Au ³⁺ 99	Ni ³⁺ 70	Cu ²⁺ 87	Ag ³⁺ 75

Table 2. Occupation energy (E_O) per defect and diffusion barrier (E_B) of the defect in different metal-doped ZnO systems.

System	Defect	E_O (eV)	Migration species	E_B (eV)
ZnO	$V_{Zn}^{2-}/V_O^0/V_O^{2+}$	/	Zn/O/O	1.4 [53]/2.36 [53]/1.7 [53]
ZnO : Ni	Ni _{Zn}	-1.79	/	/
ZnO : Cu	Cu _{Zn} /V _{Zn}	0.76	Cu _{Zn}	1.4
ZnO : Ag	Ag _{Zn} /Ag _{Zn} -V _O /Ag _{Zn} -0.5 V _O	2.86/0.26/0.42	Ag _{Zn}	0.9
ZnO : Pt	Pt _{Zn} /Pt _{Zn} -V _O	1.39/0.69	Pt _{Zn}	2.0
ZnO : Au	Au _{Zn} /Au _{Zn} -V _O	2.98/2.15	/	/

channel should account for the observed resistive switching in zinc oxide films (table S2) [39–41]. In contrast to the Ω_{LRS} , Ω_{HRS} values vary significantly (figure 3(a)). Switching devices with high work function Pt or Au as electrodes have higher Ω_{HRS} of 700 Ω –1100 Ω , while those with relatively lower work function Cu or Ag as electrodes have lower Ω_{HRS} of 100 Ω –300 Ω (table 1). Thus, the ON/OFF ratio of the M/ZnO/M devices, which decreases in the sequence of Au > Pt > Ni > Cu > Ag, is summarized in figure 3(a). Interestingly, the work function of Ni is similar to that of Pt or Au, while devices with Ni electrodes show Ω_{HRS} values close to that of the Cu or Ag electroded devices. Therefore, it could be

clarified that the work function of metal electrodes for charge carrier injection may not be the primary factor to influence the device high resistance state resistances.

Metals of Cu, Ag and Ni have low electronegativity and small ionic sizes, making them diffusible into the zinc oxide thin films [42, 43]. To evaluate the possibility of electrode metal atom migration into the switching matrix to form the conductive channels, first-principle simulation using Vienna *ab initio* simulation package [44] based on density functional theory has been performed to estimate the occupation energy of the Zn vacancies and the diffusion barrier of the electrode materials (table 2). As shown, nickel shows a negative value

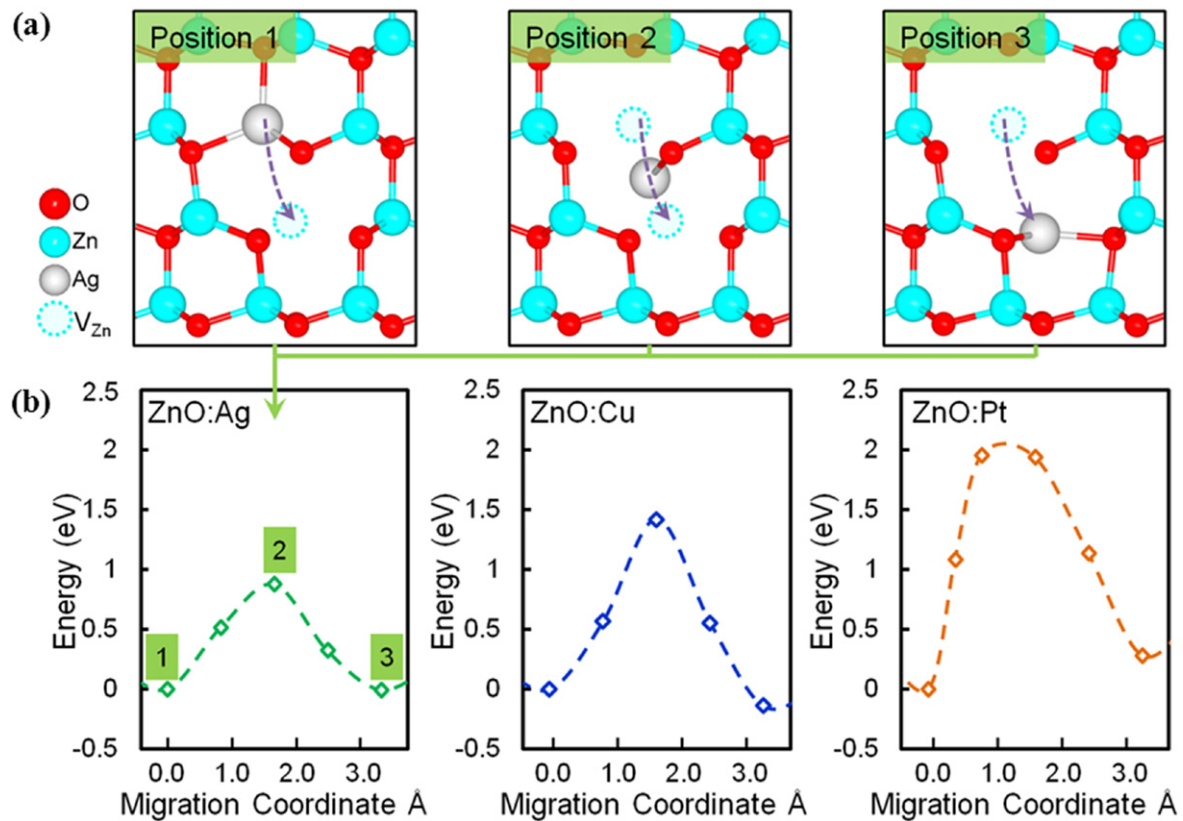


Figure 4. (a) Simulated migration path of a Ag atom in the ZnO:Ag matrix. (b) Respective calculated migration energy barriers for Ag, Cu and Pt atoms moving from the initial plane to the vacant site in the neighboring plane.

of the occupation energy, which indicates that the electrochemically oxidized Ni^{2+} species at the Ni/ZnO interface can be injected into the Zn vacancies in the switching layer spontaneously. The presence of nickel species inside the ZnO thin film is also verified by the x-ray photoelectron spectroscopic depth-profiling analysis (figure S4). Occupation of the Zn vacancies by copper and silver is slightly difficult, but is still possible when compared with platinum and gold. The diffusion barrier (0.9 eV and 1.4 eV, respectively) for Ag and Cu ions are lower than or similar to that (1.4 eV and 1.7 eV, respectively) of the Zn^{2+} and O^{2-} ions, indicating that these foreign ion species can migrate more easily in ZnO wurtzite. Figure 4 demonstrates the simulated migration path and migration energy barrier of Ag ion in ZnO matrix. Similar result has been obtained for Cu ions (not shown). Foreign active metal ions can migrate between zinc vacancy sites with relative ease. When arriving at the cathode, the foreign metal ions receive electrons from the electrode and are reduced to the metallic form. This process propagates from the cathode to the anode, and a highly conductive filament is thus formed to switch the device from the HRS to the LRS (figure 5(a)) [45, 46]. After the dissolution of the Ni, Ag or Cu filaments and resetting the device to the high resistance state by a reversed voltage, foreign ion species still exist in the switching matrix and serve as potential leaking path throughout the film, giving rise to relative lower HRS resistances. Comparably, Pt and Au are known to have relatively higher values of electronegativity, occupation energy of Zn

vacancies, ion diffusion barrier and larger ionic sizes, which prevent them from being ionized and injected into the oxide matrix to form the metallic conducting filaments [40, 41]. Therefore, the conductive path should be reasonably composed of oxygen vacancies or zinc atoms in Pt/ZnO/Pt or Au/ZnO/Au devices (figure 5(b)) [47]. When the Pt or Au electroded devices are reset to the high resistance state, a portion of the Zn atoms will be re-oxidized to ZnO form, resulting in much dilute leaking path across the film and consequently the relatively higher HRS resistances of the devices. As a larger $\Omega_{HRS}/\Omega_{LRS}$ ratio is highly desired to reduce the misreading rate for information storage applications, either platinum or gold is suggested to be used as metal electrodes. Since neither does Pt or Au participate in the solid state electrochemical formation of the conductive filaments in the present switching oxide layers, both Pt/ZnO/Pt and Au/ZnO/Au exhibit relatively better retention and endurance capability of the HRS or LRS states (figures S5 and S6). Very interestingly, conductive bridge composed of gold nanoparticles has also been observed in Au/ZnO/Au lateral structured devices, which may be arising from the unique oxide film quality, device geometry or operation methods [48].

Moreover, the set voltages of the devices with inert metal (Pt and Au) electrodes are different from that of the devices with active metal (Ni, Cu and Ag) electrodes (figure 3(b)). For instance, memory cells with Pt or Au electrodes own the set voltages (1.6 V) larger than that (0.3 V–1.1 V) of other cells with Ni, Cu or Ag electrodes, which result from the fact that

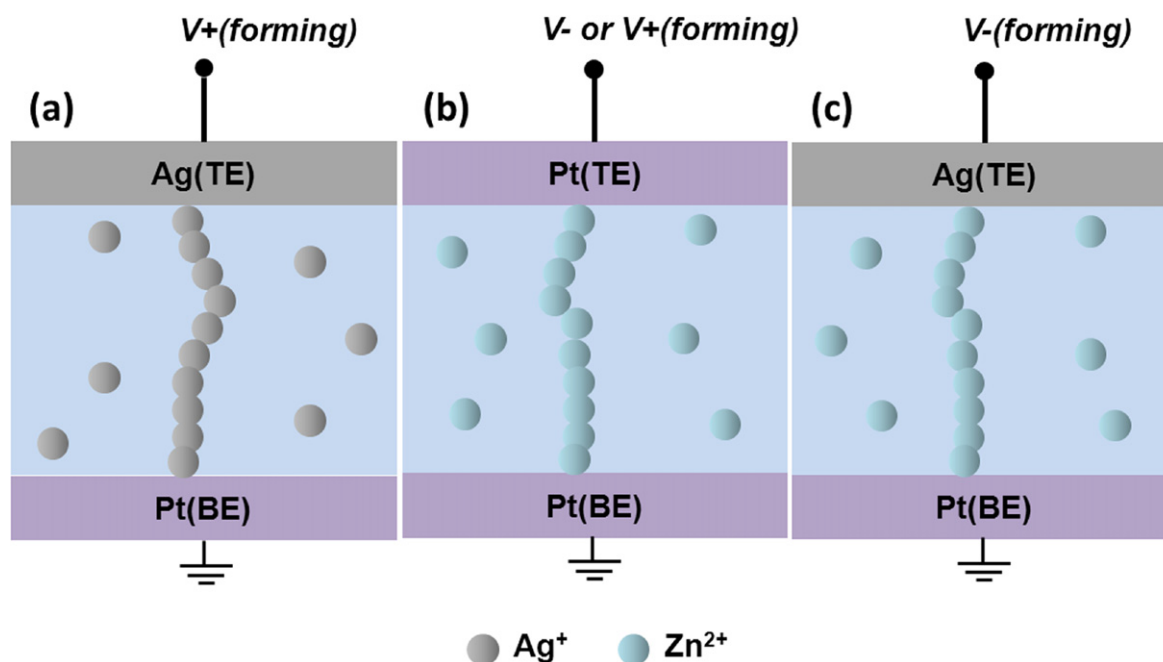


Figure 5. Schematic illustration of the Ag and Zn conduction filaments formed in the (a) Ag/ZnO/Pt device upon being subjected to the positive electroforming operation, (b) Pt/ZnO/Pt device upon being subjected to the positive or negative electroforming operation and (c) Ag/ZnO/Pt device upon being subjected to the negative electroforming operation respectively.

the formation of zinc or oxygen conduction channel is relatively more difficult than formation of Ni, Cu, or Ag filaments. On the other hand, the absolute values of the reset voltages of the switching devices, despite the electrode metals, are all comparably small (0.4 V–0.8 V), indicating that a moderate Joule heating effect is sufficient to break the metallic conduction filaments. Electrical characterization of asymmetric devices, whose BE and TE are made of different metals, can be employed to confirm the above hypothesis (table S3). In Ag/ZnO/Pt device, positive forming can easily ionize the top silver electrode and introduce Ag channels into the oxide film (figure 5(a)). Thereafter, a voltage of 1.0 V can set the device to the low resistance state. Upon resetting the device to the high resistance state, the remaining Ag species in the switching matrix lead to a lower Ω_{HRS} of 188 Ω . When the device is negatively formed, a larger set voltage of –1.7 V is required to regenerate the zinc or oxygen conduction channels (figure 5(c)). In the high resistance state, the lack of foreign metal species inevitably produces a higher Ω_{HRS} of 518 Ω . Similar results have been observed for the Pt/ZnO/Ag structure, where higher Ω_{HRS} and set voltage are found for the positive forming process, while lower Ω_{HRS} and set voltage are obtained for the negative forming process.

Beyond the work function of the metal electrodes and ion diffusion coefficients, the switching characteristics of ZnO thin film devices may also be dependent on the microstructure of both the oxide matrix and the metal/oxide interfaces. It is interesting to find that the forming voltage for Ag/ZnO/Ag device is much lower than those of the other symmetric structures (figure 3(c)). The Ag/ZnO/M asymmetric structure using Pt as the BE has significantly increased forming voltage of 6.6 V when in comparison with the Ag/ZnO/Ag structure

(tables S1 and S3). Nevertheless, with all ZnO films grown on Pt BEs exhibiting a similar roughness, the forming voltages of each individual M/ZnO/Pt devices are in the same order of magnitudes. In obvious contrast, the forming voltages of the M/ZnO/Ag devices are still small, which are 3.0 V and 2.3 V for the Pt and Cu TE devices, respectively (table S3). AFM observation suggests that the morphology of ZnO is directly related to that of the metal BEs (figure 6). For instance, ZnO films grown on relatively smoother surfaces of Pt, Au, Ni and Cu have smaller surface roughnesses of 2 nm–4 nm, while that grown on lumpy silver BE carries a much rougher topology (roughly ~ 18 nm, table S4). The uneven surface of the Ag BE is beneficial for increasing the localized electric field at the ZnO/M interfaces, which in turn enhances the metal ionization and injection or the oxygen ion migration in the switching matrix [45, 46, 49]. Consequently, the conductive filaments are formed at lower voltages in the Ag devices to turn the device to the low resistance state (figure 3(c)). The ZnO/Cu interface is less rough than the ZnO/Pt interface, resulting in the larger forming voltage of 7.1 V (table S3). Therefore, slightly rougher interface is desired to reduce the device forming voltage, power consumption and potential risk of permanent breakdown.

4. Summary

In this work, a systematic investigation has been performed to study the influence of metal electrodes on the resistive switching properties of zinc oxide films. It is found that neither does any single factor of the atomic order, the work function nor the electronegativity can determine all the

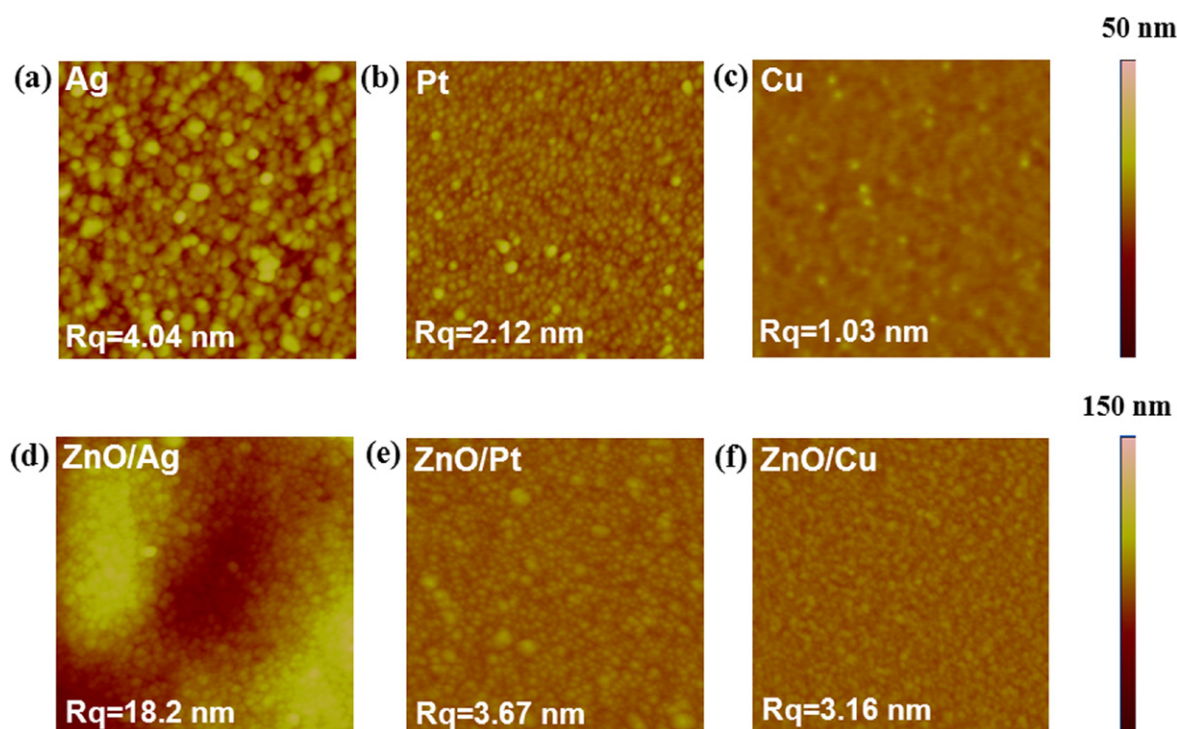


Figure 6. AFM images of the (a) bare Ag (b) Pt and (c) Cu substrates, and ZnO films grown on (d) Ag (e) Pt and (f) Cu substrates, respectively. The scanning areas are maintained at $2\ \mu\text{m} \times 2\ \mu\text{m}$.

switching parameters including the device resistances in the HRS and LRS, the ON/OFF ratios, the setting and resetting voltages, as well as the forming voltages of the M/ZnO/M devices with different electrode metals. Instead, it is the synergistic interplay between the work function, electro-negativity, ionic size of the electrode metals, as well as the roughness of the ZnO/M interfaces, that influence the resistive switching behaviors of the ZnO based RRAM devices. Regardless of the choice of electrode metals, all the M/ZnO/M structure devices demonstrate metallic conduction behavior in the low resistance states. Formation of localized conduction channels composed of electrode metals or zinc/oxygen atoms is considered responsible for the observed filamentary conduction behavior. Due to the lack of foreign metallic species as the leaking sites in the Pt or Au devices, Pt/ZnO/Pt and Au/ZnO/Pt structures possess higher Ω_{HRS} and set voltage values. In contrast, devices with Ni, Cu and Ag electrodes show lower Ω_{HRS} and set voltage values. Since moderate energy is sufficient to thermally disrupt the metallic filaments, all the devices have similar low reset voltages of $\sim \pm 0.5\ \text{V}$. Rougher surfaces also assist the formation of conductive filaments, and thus is beneficial for lowering the forming voltages of the ZnO switching devices.

Acknowledgments

This work was supported by the State Key Research Program of China (973 Program, 2012CB933004), National Natural Science Foundation of China (51025101, 11274321, 51303194, 61328402, 61306152), the Youth Innovation

Promotion Association of the Chinese Academy of Sciences, Ningbo Natural Science Foundations (2013A610031), and Science and Technology Innovative Research Team of Ningbo Municipality (2009B21005, 2011B82004).

References

- [1] Waser R and Aono M 2007 *Nat. Mater.* **6** 833–40
- [2] Akinaga H and Shima H 2010 *Proc. IEEE* **98** 2237–51
- [3] Yang J J, Strukov D B and Stewart D R 2013 *Nat. Nanotechnology* **8** 13–24
- [4] Sakamoto T, Lister K, Banno N, Hasegawa T, Terabe K and Aono M 2007 *Appl. Phys. Lett.* **91** 092110
- [5] Pickett M D, Strukov D B, Borghetti J L, Yang J J, Snider G S, Stewart D R and Williams R S 2009 *J. Appl. Phys.* **106** 074508
- [6] Seo S *et al* 2004 *Appl. Phys. Lett.* **85** 5655
- [7] Yang Y, Gao P, Gaba S, Chang T, Pan X and Lu W 2012 *Nat. Commun.* **3** 732
- [8] Yang J J, Pickett M D, Li X M, Ohlberg D A A, Stewart D R and Williams R S 2008 *Nat. Nanotechnology* **3** 429–33
- [9] Yang J J, Strachan J P, Miao F, Zhang M X, Pickett M D, Yi W, Ohlberg D A A, Ribeiro G M and Williams R S 2011 *Appl. Phys. A* **102** 785–9
- [10] Zhao J-L, Li X-M, Bian J-M, Yu W-D and Gao X-D 2005 *J. Cryst. Growth* **276** 507–12
- [11] Yang Y, Long H, Yang G, Chen A, Zheng Q and Lu P 2009 *Vacuum* **83** 892–6
- [12] Chen A, Bi Z, Tsai C-F, Lee J H, Su Q, Zhang X, Jia Q, MacManus-Driscoll J L and Wang H 2011 *Adv. Funct. Mater.* **21** 2423–9
- [13] Xu N, Liu L F, Sun X, Liu X Y and Han D D 2008 *Appl. Phys. Lett.* **92** 232112

- [14] Chang W Y, Lai Y C, Wu T B, Wang S F, Chen F and Tsai M J 2008 *Appl. Phys. Lett.* **92** 022110
- [15] Chang W Y, Lin C A, He J H and Wu T B 2010 *Appl. Phys. Lett.* **96** 242109
- [16] Lee S, Kim H, Park J and Yong K 2010 *J. Appl. Phys.* **108** 076101
- [17] Yang Y C, Zhang X X, Gao M, Zeng F, Zhou W Y, Xie S S and Pan F 2011 *Nanoscale* **3** 1917–21
- [18] Qi J, Olmedo M, Ren J J, Zhan N, Zhao J Z, Zheng J G and Liu J L 2012 *ACS Nano* **6** 1051–8
- [19] Qi J, Olmedo M, Zheng J G and Liu J L 2013 *Sci. Rep.* **3** 2405
- [20] Zhang J, Yang H, Zhang Q L, Dong S R and Luo J K 2013 *Appl. Phys. Lett.* **102** 012113
- [21] Villafuerte M, Heluani S P, Juárez G, Simonelli G and Braunstein G 2007 *Appl. Phys. Lett.* **90** 052105
- [22] Qiu J, Shih A, Zhou W D, Mi Z T and Shih I 2011 *J. Appl. Phys.* **110** 014513
- [23] Zhu G F, Peng S S, He C L, Zhu X J, Chen X X, Liu Y W and Li R-W 2011 *Nanotechnology* **22** 275204
- [24] Chang W Y, Huang H W, Wang W T, Hou C H, Chueh Y L and Hea J H 2012 *J. Electrochem. Soc.* **159** G29–32
- [25] Tang M H, Jiang B, Xiao Y G, Zeng Z Q, Wang Z P, Li J C and He J 2012 *Microelectron. Eng.* **93** 35–8
- [26] Peng H Y, Li G P, Ye J Y, Wei Z P and Zhang Z 2010 *Appl. Phys. Lett.* **96** 192113
- [27] Shi L, Shang D S, Chen Y S, Wang J, Sun J R and Shen B G 2011 *J. Phys. D: Appl. Phys.* **44** 455305
- [28] Wang Z Q, Xu H Y, Zhang L, Li X H, Ma J G, Zhang X T and Liu Y C 2013 *Nanoscale* **5** 4490–4
- [29] Russo U, Cagli C, Spiga S, Cianci E and Ielmini D 2009 *Electron. Dev. Lett.* **30** 817–9
- [30] Chen M C, Chang T C, Tsai C T, Huang S Y, Chen S C, Hu C W, Sze S M and Tsai M J 2010 *Appl. Phys. Lett.* **96** 262110
- [31] Bertaud T *et al* 2012 *Thin Solid Films* **520** 4551–5
- [32] Cabout T, Buckley J, Cagli C, Jousseau V, Nodin J-F, de Salvo B, Bocquet M and Muller Ch 2013 *Thin Solid Films* **533** 19–23
- [33] Hu Y S, Perello D, Yun M, Kwon D H and Kim M 2013 *Microelectron. Eng.* **104** 42–7
- [34] Jeong H Y, Kim S K, Lee J Y and Choi S Y 2011 *Electrochem. Soc.* **158** H979–82
- [35] Zhuo V Y Q, Jiang Y, Li M H, Chua E K and Zhang Z 2013 *Appl. Phys. Lett.* **102** 062106
- [36] Peng S S, Zhu G F, Chen X X, Zhu X J, Hu B L, Pan L, Chen B and Li R-W 2012 *Appl. Phys. Lett.* **100** 072101
- [37] Zhu X J, Su W J, Liu Y W, Hu B L, Pan L, Lu W, Zhang J D and Li R-W 2012 *Adv. Mater.* **24** 3941–6
- [38] Philip Wong H-S, Lee H-Y, Yu S, Chen Y-S, Wu Y, Chen P S, Lee B Y, Chen F T and Tsai M-J 2012 *Proc. IEEE* **100** 1950–70
- [39] Yang Y C, Pan F, Liu Q, Liu M and Zeng F 2009 *Nano Lett.* **9** 1636–43
- [40] Huang Y T *et al* 2013 *Anal. Chem.* **85** 3955–60
- [41] Chen J Y, Hsin C L, Huang C W, Chiu C H, Huang Y T, Lin S J, Wu W W and Chen L J 2013 *Nano Lett.* **13** 3671–7
- [42] Sun J *et al* 2013 *Appl. Phys. Lett.* **102** 053502
- [43] Wu X, Cha D, Bosman M, Raghavan N, Migas D B, Borisenko V E, Zhang X X, Li K and Pey K-L 2013 *J. Appl. Phys.* **113** 114503
- [44] Kresse G and Furthmüller J 1996 *Phys. Rev. B* **54** 11169–86
- [45] Liu Q, Long S, Lv H, Wang W, Niu J, Huo Z, Chen J and Liu M 2010 *ACS Nano* **4** 6162–8
- [46] Wang Z Q, Xu H Y, Zhang L, Li X H, Ma J G, Zhang X T and Liu Y C 2013 *Nanoscale* **5** 4490
- [47] Shang J, Liu G, Yang H L, Zhu X J, Chen X X, Tan H W, Hu B L, Pan L, Xue W H and Li R-W 2014 *Adv. Funct. Mater.* **24** 2171
- [48] Peng C-N, Wang C-W, Chan T-C, Chang W-Y, Wang Y-C, Tsai H-W, Wu W-W, Chen L-J and Chueh Y-L 2012 *Nanoscale Res. Lett.* **7** 559
- [49] Verrelli E, Tsoukalas D, Normand P, Kean A H and Boukos N 2013 *Appl. Phys. Lett.* **102** 022909
- [50] Pauling L 1960 The nature of the chemical bond and the structure of molecules and crystals *An Introduction to Modern Structural Chemistry* (Ithaca, NY: Cornell University Press) p 272
- [51] Michaelson H B 1977 *J. Appl. Phys.* **48** 4729
- [52] Shannon R D 1976 *Acta. Cryst. A* **32** 751–67
- [53] Janotti A and Van de Walle C G 2007 *Phys. Rev. B* **76** 165202